Mechanism of RNA 2′-O-Methylation: Evidence that the Catalytic Lysine Acts To Steer Rather than Deprotonate the Target Nucleophile†

C. Li,‡ Y. Xia,§ X. Gao,§ and P. D. Gershon*,‡

Department of Medical Biochemistry and Genetics/Institute of Biosciences and Technology, Texas A&M University System Health Science Center, Houston, Texas 77030, and Department of Chemistry, University of Houston, 136 Fleming Street, Houston, Texas 77204-5003

Received November 8, 2003; Revised Manuscript Received February 19, 2004

ABSTRACT: The weight of current evidence suggests that RNA 2′-*O*-MTases employ an S_N2 mechanism with an in-line attack of the target nucleophile upon the methyl group of the AdoMet cofactor. It has been suggested that, like the phosphohydrolytic enzymes, ribozymes, and nucleic acid polymerases, the RNA 2′-*O*-MTases initially activate the substrate's attacking hydroxyl oxygen by deprotonation. Here, evidence is presented that the vaccinia virus mRNA cap specific 2′-*O*-MTase VP39 does not promote RNA 2′-oxyanion formation but that instead it acts by steering a hydroxyl oxygen orbital toward the cofactor methyl center.

The common role of the AdoMet-dependent MTases[1] is to catalyze the transfer of AdoMet's methyl group to an acceptor atom (*1*). Although methylatable acceptors are found within a variety of molecular classes, including nucleic acids, proteins, lipids, polysaccharides, and small molecules, much of this diversity in MTase target atoms is reflected in one species of acceptor, namely, RNA [tRNA, for example, contains among its repertoire of methylated nucleosides N7-methylguanosine, N1-methylguanosine, N1-methyladenosine, C5-methyluridine, C2-methyladenosine, and 2′-*O*-methyladenosine (*2*)]. RNA 2′-O-methylation is of interest at present due in large part to its key role in rRNA biogenesis and function and the unusual mechanism by which 2′-O-methylation sites are targeted within the rRNA via highly tailored small nuclear RNA (snoRNA) guides (*3*−*6*). Despite the widespread occurrence of 2′-O-methylation in tRNA, rRNA, and mRNA, the catalytic mechanism of RNA 2′-O-methylation has not been characterized at the atomic level.

For nucleophilic methyl acceptors such as oxygen, the most parsimonious mechanism for the transfer of methyl groups from AdoMet seems to be a relatively straightforward S_N2 one in which attack by an electron lone pair of the nucleophile upon the methyl leads, in the transition state, to a linear arrangement of the nucleophile, the methyl carbon, and the thioester leaving group followed by the completion of methyl transfer and stereochemical inversion of the methyl. For oxygen methyl acceptors, does the initial attack require prior formation of a 2′-oxyanion? Ribose oxyanion formation is reported to play a pivotal role in preparation for nucleophilic attack upon a phosphoryl center in other enzyme and ribozyme systems. For example, the initial step in RNAse A-catalyzed RNA hydrolysis appears to involve attack by the O2′ adjacent to the scissile phosphodiester in its 2′-oxyanion form (*7*). For nucleic acid polymerases, high-resolution crystal structures have indicated the occurrence of proton transfer from the attacking primer 3′-OH to an acidic side chain [assisted by an O3′-coordinated metal acting as a Lewis acid (refs *8* and *9* and references therein)]. A similar role for metal activation of the attacking ribose alkoxide has been proposed for phosphohydrolytic ribozymes [with loss of protons to the solvent (*10*−*12*)] and for activation of the serine hydroxyl of alkaline phosphatase (*13*).

With regard to enzyme-catalyzed *O*-methyl transfer, clear evidence for general base catalysis or oxyanion formation has not been provided as far as we are aware. COMT (*14*) is a reasonable candidate for an *O*-MTase whose attacking nucleophile might be an oxyanion insofar as an Mg^{2+} ion lies close to its reaction center in the cocrystal structure of enzyme, AdoMet cofactor, and substrate analogue, suitably positioned to promote hydroxyl deprotonation (*15*, *16*). Moreover, the pK_a for the first of the two hydroxyl ionizations in catechol (the COMT substrate) is only 9.34 (*17*). These factors notwithstanding, it is not clear that substrate hydroxyl deprotonation status has been addressed for COMT.

In contrast to the aromatic character of catechol's two vicinal target hydroxyls, the target of RNA 2′-O-methylation is an aliphatic hydroxyl. The 2′-hydroxyls of RNA (as well as other aliphatic hydroxyls) typically exhibit pK_a values greater than ∼12.2 (refs *18* and *19* and references therein). With regard to the necessity of 2′-oxyanion formation, perhaps the only available paradigm is that of low-molecular weight model compounds (*20*, *21*). The *in vitro* study of these has indicated that intramolecular nucleophilic attack of a hydroxyl oxygen upon the sp^3-hybridized methyl carbon

† This work was supported by NSF Grants MCB-9604188 and MCB-0091260.

* To whom correspondence should be addressed: Rm. 817, IBT, 2121 W. Holcombe Blvd., Houston, TX 77030. Telephone: (713) 677-7665. Fax: (713) 677-7689. E-mail: pgershon@ibt.tamhsc.edu.

‡ Texas A&M University System Health Science Center.

§ University of Houston.

[1] Abbreviations: MTase, methyltransferase; AdoMet, *S*-adenosylmethionine; AdoHcy, *S*-adenosylhomocysteine; COMT, catechol *O*-MTase.

10.1021/bi0359980 CCC: $27.50
Published on Web 04/23/2004

attached to a trivalent sulfonium center is base-catalyzed, strongly implicating deprotonation of the hydroxyl nucleophile as a prerequisite for the reaction.

Vaccinia virus protein VP39 is an RNA 2′-*O*-MTase which functions at the 5′ ends of N^7mG-capped mRNAs by 2′-O-methylation of the 5′-most transcribed nucleotide (*22*−*24*). VP39 has provided a prototypical gene for a nucleic acid 2′-*O*-MTase (*24*) and a prototypical three-dimensional (3D) structure for a nucleic acid sugar specific MTase (*25*, *26*). Although the structures of other RNA 2′-*O*-MTases (e.g., FtsJ/RrmJ, RlmB, flavivirus NS5, and the Reovirus core) have more recently been reported (*27*−*32*), the only 3D view of a 2′-*O*-MTase catalytic center with a bound RNA substrate and cofactor reported thus far is that of VP39 (*33*). Although VP39 is functionally related to COMT insofar as it also methylates a hydroxyl oxygen, VP39 is unrelated not only in targeting an aliphatic hydroxyl but also in having a catalytic mechanism that is entirely metal ion-independent. Factors that might permit a general base-catalyzed mechanism for VP39 are therefore much less apparent than for COMT.

To address experimentally whether VP39's catalytic mechanism includes a 2′-oxyanion formation step, we have used two-dimensional (2D) NMR techniques to probe for enzyme-dependent and pH-dependent change in the ionization status of VP39's RNA substrate in the context of the substrate−enzyme−cofactor complex.

EXPERIMENTAL PROCEDURES

Synthesis and Purification of N^7mG(5′)ppp[^{13}C]G. N^7mG(5′)ppp[^{13}C]G (cap dinucleotide specifically ^{13}C-enriched at the unmethylated guanosine) was synthesized by N7-methylation and morpholination of guanosine diphosphate, followed by its condensation with uniformly ^{13}C-enriched (98%) guanosine monophosphate (Martek Co.) according to ref *34*. The product was purified over a DEAE-Sephadex A25 column as described previously (*34*). After N^7mG(5′)ppp[^{13}C]G-containing fractions had been pooled and dried followed by sodiation (*34*), ∼20 aliquots of the product were sequentially injected into an analytical C_{18} reverse phase column [Vydac; buffer A consisting of 0.1 M triethylamine acetate (TEAA) at pH 5.8 and buffer B consisting of 0.1 M TEAA and 25% CH_3CN at pH 5.8]. Each injection was followed by a two-part gradient: 0 to 15% B from 0 to 10 min and 15 to 60% B from 10 to 120 min (1 mL/min). The major peak from each run (eluting at ∼12 min) was dried by vacuum centrifugation and redissolved in water.

Synthesis and Purification of N^7mG(5′)ppp[^{13}C]G(sA)$_3$. The RNA N^7mG(5′)ppp[^{13}C]G(sA)$_3$ (where sA represents phosphorothioadenosine monophosphate; RNA henceforth abbreviated as [^{13}C]G-RNA) was synthesized by runoff T7 transcription of a partially double-stranded oligonucleotide template in the presence of N^7mG(5′)ppp[^{13}C]G (above) and phosphorothioadenosine triphosphate as described previously (*33*−*35*). Newly synthesized RNA was purified as described previously (*34*), except that in some instances a semipreparative scale C_{18} column was used in combination with a gradient of 3.75 to 15.6% CH_3CN in 0.1 M TEAA (pH 5.75, overall gradient volume of 130 mL, 1 mL/min). Fractions containing [^{13}C]G-RNA were pooled and dried under vacuum. The RNA was redissolved in heat-sterilized 50 mM sodium phosphate (pH 7.4) to a concentration of ∼1.5−2 mM and quantitated by absorption at 260 nm. Immediately prior to NMR experiments, it was supplemented with sufficient solid $(NH_4)_2SO_4$ to yield a final concentration of 250 mM of the latter after mixing with protein (below).

Protein Expression and Purification. Rosetta(DE3) *Escherichia coli* (Novagen, Inc.) containing plasmid ΔCHis (A. E. Hodel, unpublished work; a pET28a clone of the VP39-ΔC32 coding sequence C-terminally tagged with six histidine codons) was grown at 37 °C overnight in 4 L of superbroth containing 30 mg/L kanamycin, after which 0.4 mM IPTG was added and the culture incubated for an additional 3 h at 37 °C. After being harvested by centrifugation, cells were lysed in 10 mM HEPES-NaOH (pH 8.0), 5 mM 2-mercaptoethanol, 250 mM NaCl, and 10% glycerol. The lysate was supplemented with $MgCl_2$ to a final concentration of 1 mM and treated with DNAase I (1 unit/mL of extract) at room temperature for 15 min. After sonication on ice (15 × 20 s) followed by centrifugation (30 min at 13000*g* and 4 °C), the supernatant was applied to a column containing 20 mL of NiNTA Superflow resin (Qiagen, Inc.) pre-equilibrated in buffer A [50 mM sodium phosphate and 250 mM NaCl (pH 7.4)] at a flow rate of 2 mL/min. After the column had been washed with ∼1.5−2 L of buffer A containing 10 mM imidazole-HCl until no RNAse activity could be detected in the eluent (RNAse alert kit, Ambion Inc.), the protein was eluted with a linear 120 mL gradient of buffer A containing 50 to 250 mM imidazole-HCl at a flow rate of 2 mL/min and then stored at 4 °C.

A K175C mutation was generated in a plasmid containing the coding sequence for GST-VP39(cys$^-$) (*36*) as described elsewhere (manuscript in preparation), after which the 6His-VP39(cys$^-$)-K175C sequence was recloned as an *Nco*I−*Hin*dII fragment in plasmid pET30a (Novagen Inc.) followed by expression and purification as described above, except that protein expression was induced at 23 °C.

Prior to use in NMR experiments, VP39-ΔC32-6His and 6His-VP39(cys$^-$)-K175C (henceforth termed VP39 and VP39-K175C, respectively) were exchanged into NMR buffer [50 mM sodium phosphate, 50 mM NaCl, and 0.5% sodium azide (pH 7.4), heat-sterilized] and concentrated to 0.4 mM by ultrafiltration (PL-10, 10K NMWL, Millipore). The protein concentration was quantitated by absorption at 280 nm (1 OD_{280} = 0.93 mg/mL). The resulting protein preparations were stored at 4 °C for short periods. Aliquots were carefully tested for the absence of RNAse activity as described in the Supporting Information. Preparations showing no significant RNA degradation or loss of MTase activity were used for NMR experiments (below).

NMR Spectroscopy. ^{13}C-enriched phenol (Cambridge Isotope Laboratories) was dissolved in 50 mM sodium phosphate and 50 mM NaCl (pH 7.5) at a concentration of 3.45 mM. ^{13}C-enriched guanosine 5′-monophosphate (5′-rGMP, Spectrum Stable Isotopes, Columbia, MD) was dissolved in 50 mM sodium phosphate and 50 mM NaCl (pH 7.5) at a concentration of 5.36 mM. Sample volumes were 0.6 mL.

For all [^{13}C]G-RNA-containing NMR experiments, pH-adjusted, D_2O-supplemented protein samples were mixed with $(NH_4)_2SO_4$-supplemented [^{13}C]G-RNA as described above (Protein Expression and Purification) and then further supplemented where appropriate with either the cofactor

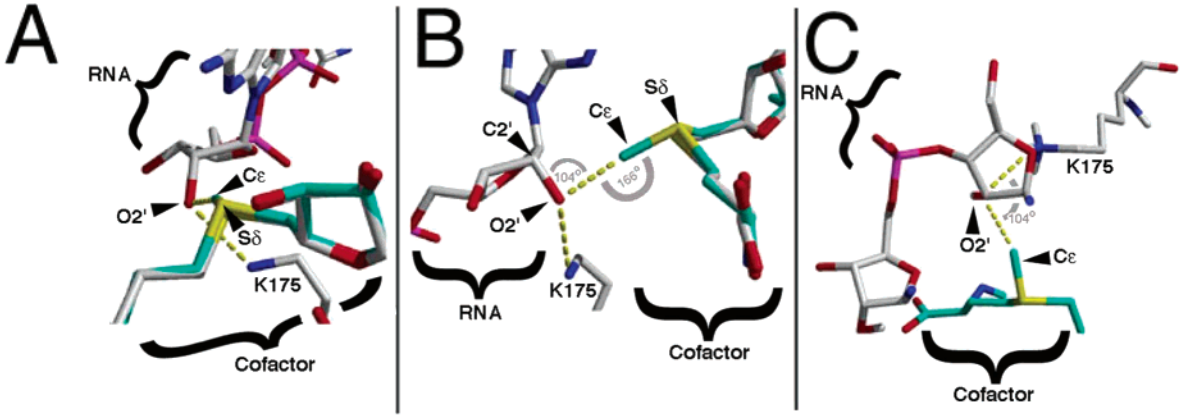

FIGURE 1: VP39's MTase catalytic center viewed from three angles [red for oxygen, blue for nitrogen, purple for phosphorus, yellow for sulfur, gray and green (cofactor) or gray (other) for carbon] with the cofactor methyl added *in silico* (*33*). (A) View with the AdoMet Cϵ−Sδ bond pointing into the page. (B) View in the plane made up of the ribose C2′−O2′ bond, the O2′−Cϵ putative hydrogen bond, and the AdoMet Cϵ−Sδ bond. Other details are as described for panel A. (C) View with the ribose C2′−O2′ bond pointing into the page.

(AdoMet) or the cofactor product (AdoHcy) to final concentrations of 0.4 mM. Final sample volumes were 0.6−0.7 mL. During experiments, upward pH titration was carried out by the stepwise addition of 2 M NaOD in D_2O (2−4 μL per pH point) with gentle mixing, and the pH was monitored using a pH microprobe (model MI-710, Microprobes, Inc.).

All spectra were acquired at 295 K using a Bruker Avance 600 MHz NMR spectrometer in heat-sterilized NMR tubes. All chemical shift (δ) values were referenced with respect to an internal (initial experiments) standard comprising 2,2-dimethyl-2-silapentane-5-sulfonic acid (0.0 ppm). In later experiments, the prior internal reference data served as an external reference. Water solvent suppression was applied for all 2D experiments. ^{13}C-enriched phenol and 5′-rGMP were subjected to one-dimensional NMR (1D sequence "zgpr" with f_1 presaturation), titrating with 2 M NaOD up to pH ∼13.0 (acquisition time per spectrum of ∼30 min). The highest pH point (pD 14.0) was generated separately by dissolving 5′-rGMP directly in 1.0 M NaOD.

Protein and RNA samples were examined using 2D ^{13}C−^{1}H HSQC (sequence "Chsqc" with purge pulse p28 and spin lock p27 for water suppression). Conditions for the acquisition of the NMR spectra for [^{13}C]G-RNA-containing samples were as described in the Supporting Information. For each pH titration experiment, six data sets (corresponding to the six pH points) were recorded over a 48 h period, samples being stored overnight at 4 °C when not in the spectrometer. After spectroscopy and prior to RNA re-isolation, samples were stored at −20 °C, for up to several weeks.

RNA Re-Isolation and Recycling. After each series of HSQC spectra was recorded, [^{13}C]G-RNA-containing samples were re-isolated from NMR samples by supplementing to a final volume of 1.0 mL with HPLC buffer A (above) without added ammonium sulfate and, after a brief centrifugation, subjecting the supernatant to semipreparative C_{18} column chromatography as described above [Synthesis and Purification of N^{7}mG(5′)ppp[^{13}C]G(sA)$_3$]. Peaks corresponding to intact, recovered [^{13}C]G-RNA were identified by MALDI-TOF mass spectrometry (Supporting Information), and the corresponding dried fractions were supplemented with (typically an ∼4-fold excess of) freshly transcribed and purified [^{13}C]G-RNA for the subsequent NMR experiment.

K_m values were identified as described previously (*37*).

RESULTS

VP39's Catalytic Center. Inspection of the 3D structure of VP39's catalytic center with a bound RNA substrate and an AdoHcy cofactor product (*33*) (Figure 1) shows the reaction components to be suitably arranged for an in-line S_N2 reaction in which a lone pair of the substrate's nucleophilic ribose O2′ can attack AdoMet's methyl group, leading to the expulsion of AdoHcy. The side chain of residue K175 is appropriately oriented to play a role in the preparation of the initial O2′ nucleophile by deprotonating it or fixing its orientation.

The mechanism described above is supported not only in the arrangement and mutual distances of components but also in the bond angles. Thus, the modeled Sδ−Cϵ bond of AdoMet (where Sδ and Cϵ are AdoMet's sulfur and donor methyl carbon, respectively) points almost directly at the target ribose O2′ (Figure 1A). Specifically, AdoMet's Sδ−Cϵ bond subtends an angle of 166° with the putative hydrogen bond between AdoMet's Cϵ and the ribose O2′ (Figure 1B). This is very close to the value of 180° that would be ideal for S_N2 in-line attack upon AdoMet's Cϵ by the O2′ lone pair. In addition, the ribose C2′−O2′ bond subtends an angle of 104° with the O2′−AdoMet Cϵ putative hydrogen bond (Figure 1B), which is appropriate for nucleophilic attack by the O2′ lone pair upon AdoMet's Cϵ (for a perfect tetrahedron, this angle would be 109°; for the oxygen of H_2O, the equivalent hydrogen bonding angle is also 104°). Finally, K175's Nϵ and AdoMet's Cϵ subtend an angle of 104° about the target ribose O2′ (Figure 1C). Thus, with a ribose O2′ lone pair pointing at AdoMet's Cϵ for nucleophilic attack, the O2′−H bond of the hydroxyl (protonated or otherwise) could point directly at Nϵ of K175. The catalytic center therefore seems to be well poised for an in-line S_N2 attack of the resulting ribose 2′-hydroxyl oxygen upon Cϵ of AdoMet. Although the crystal structure shown in Figure 1 was obtained with AdoHcy as opposed to AdoMet in the cofactor pocket (*33*), the location and orientation of the bound AdoHcy were indistinguishable from that of bound AdoMet in the earlier structure of the enzyme−AdoMet binary complex (*26*), and the donor methyl in Figure 1 was modeled according to the earlier structure.

NMR for the Detection of Hydroxyl Deprotonation. To confirm the sensitivity of NMR to hydroxyl deprotonation

by upward pH titration, ^{13}C-labeled phenol (a prototypical hydroxylated aromatic compound with a moderate pK_a) was subjected to 1D NMR, titrating the pH from 6.0 to 13.0 while recording 1D ^{13}C spectra at intervening pH values. A downfield change in the coalesced signal of δ for phenol's 1-^{13}C as a function of pH was clearly detectable (Figure 2A), corresponding to the known pK_a for phenol of ~9.95 (*17*) and the direction of δ migration previously observed upon deprotonation of aliphatic carbon substituents (*38*, *39*).

Ribose carbons of ^{13}C-enriched 5′-rGMP, a direct precursor of the [^{13}C]G-RNA substrate for VP39 (below), were next examined for pH-dependent 2′-OH deprotonation, as an indication of the magnitude and direction of spectral change that might be expected upon enzymatic activation of the same moiety within RNA. Titration and 1D NMR monitoring (Figure 2B) indicated two transitions with increasing pH, namely, (a) an upfield migration of δ with a transition point at pH ~10.0 (most noticeable at C1′) corresponding to the known pK_a of 5′-rGMP's N1 proton of 10.0 (*40*) and (b) a downfield change in δ with a transition point at pH ~12.25 (most noticeable at C2′). The latter value corresponded well with reported pK_a values of ~12.2−13.6 for the 2′-OH moieties of various nucleosides, nucleoside 3′-monophosphates, and 3′,5′-bisalkyl phosphodiester derivatives (*18*). The magnitude of the pH-dependent change in δ at C2′ of 5′-rGMP (~1.5 ppm, Figure 2B) was less dramatic than that recorded for [^{13}C]phenol (~10 ppm) presumably because of the inductive capacity of phenol's conjugated ring.

Nucleobase functional groups within phosphohydrolytic ribozymes have previously been examined using 1D NMR techniques (*41*). To maximize sensitivity and resolution, we chose to use 2D (^{1}H−^{13}C correlation) spectroscopy for our examination of the ribose carbons of [^{13}C]G-RNA (Figure 3, below). In a preliminary HSQC spectrum of the [^{13}C]-rGMP precursor (Figure 2C), the ^{13}C−^{1}H coupling peaks corresponding to the ribose carbons were each clearly resolved from one another and from spectral peaks for the guanine base. Cross-peaks were assigned to the individual carbons according to the characteristic connectivities of the corresponding protons (*42*).

Insensitivity of the RNA 2′-OH to pH in the Context of VP39. Synthesis of the ^{13}C-enriched N^{7}mGpppG dinucleotide mRNA cap analogue and its incorporation into [^{13}C]G-RNA are described in the Supporting Information. This RNA was identical in both molecular structure and phosphorothio substitution status to the VP39-bound portion of the cocrystallized RNA in the VP39-AdoHcy-capped RNA cocrystal structure (Figure 1; *33*); it differed in only the isotope enrichment status. At each of six pH points in the range of 6.25−8.6 [encompassing the pH optimum of VP39's MTase activity (*22*) and over which VP39's native conformation should be preserved], ^{13}C−^{1}H HSQC spectra were generated for the following samples in the following order: (a) [^{13}C]G-RNA alone (control), (b) [^{13}C]G-RNA with wild-type VP39 (1:1 complex; to determine whether VP39 promotes deprotonation of the RNA 2′-OH), (c) [^{13}C]G-RNA with wild-type VP39 and AdoHcy (1:1:1 complex), and (d) [^{13}C]G-RNA with VP39-K175C and AdoMet (1:1:1 complex). Samples c and d aimed to mimic a reaction complex "poised" just prior to methylation, via omission of either the AdoMet CH_3 (sample c) or the terminal ethylamine of the K175 side chain (sample d). The inclusion of AdoHcy in sample c not

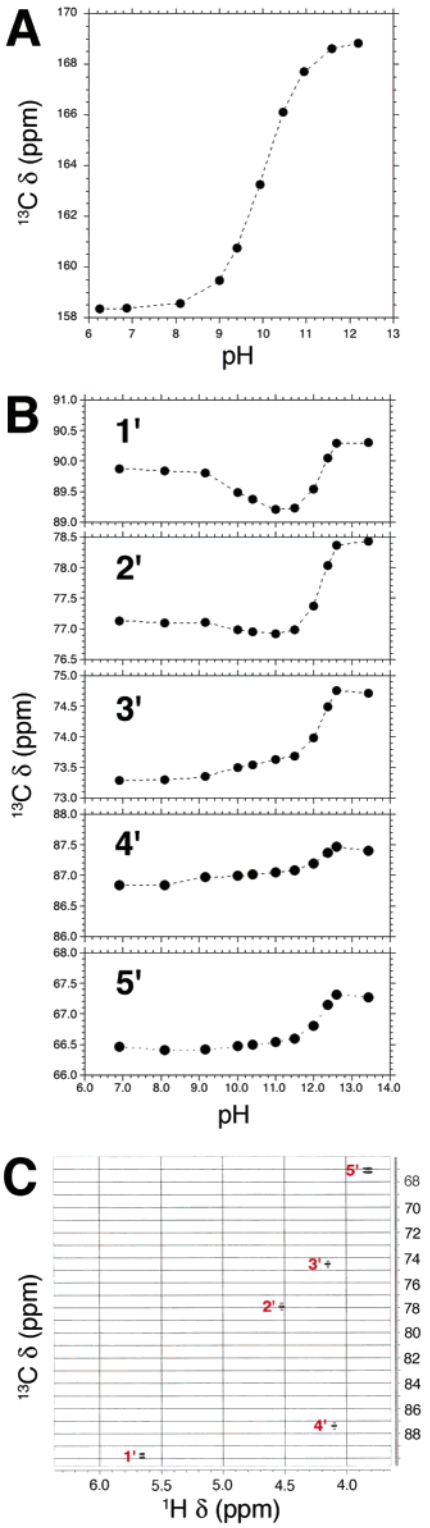

FIGURE 2: pH-dependent deprotonation detected by 1D and 2D NMR. (A) 1-^{13}C of phenol. pH titration of δ by 1D NMR. (B) Ribose ^{13}C atoms of ^{13}C-enriched 5′-rGMP. pH titration of δ by 1D NMR (pH inferred from pD by the relationship pH = pD − 0.4). Deprotonation of C2′ and C3′ hydroxyls over the pH range of 11.5−12.6 was detected directly, while coordinated but smaller (secondary) changes at the other ribose carbons resulted from inductive and through-space effects (*38*, *39*). The secondary response was more pronounced at C1′ than at C4′ and C5′ because of the O4′−C1′−N1 anomeric effect [which arises at elevated pH due to the increased aromaticity of the guanuin-9-yl moiety resulting from N1 deprotonation (*52*)]. (C) 2D (HSQC) spectrum for ^{13}C-enriched 5′-rGMP at pH 6.0, showing ribose (1′−5′) C−H assignments.

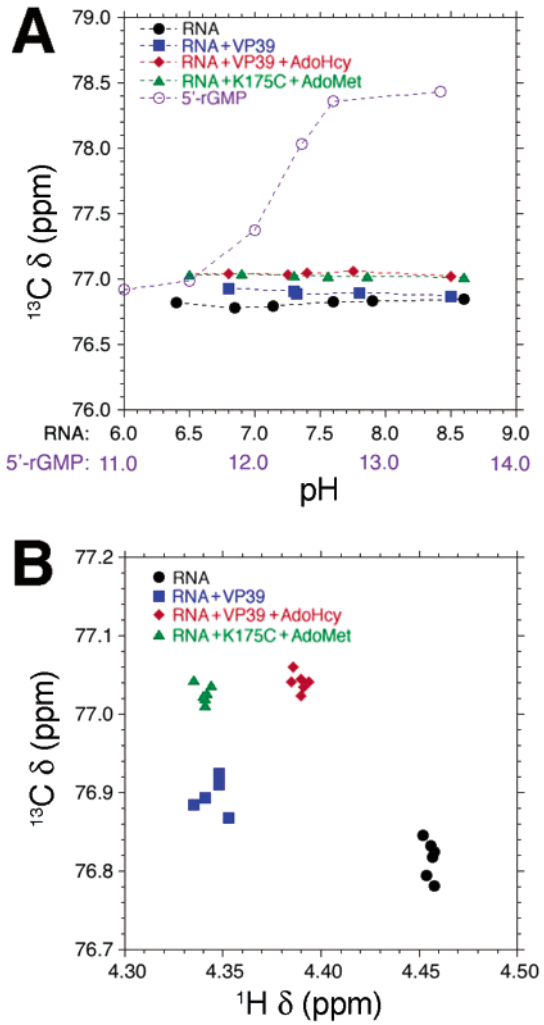

FIGURE 3: pH 6.25−8.60 titration of [^{13}C]G-RNA, in four samples: RNA alone, RNA with VP39, RNA with VP39 and AdoHcy, and RNA with VP39-K175C and AdoMet. In the protein-containing samples, the RNA:protein stoichiometry was 1:1 (forward-capped RNA:protein stoichiometry being <1:1). (A) pH vs δ for the RNA's target ^{13}C2′. For comparison, the pH 11.0−14.0 titration for C2′ of 5′-rGMP (from Figure 2B) is overlaid. (B) Data points from panel A plotted against ^{1}H δ values from the same HSQC spectra.

only ensured that the conformation and microenvironment of the catalytic center reflected the active (cofactor-bound) ones as closely as possible but also reflected the inclusion of this compound in the crystallographic study (Figure 1; *33*). Moreover, the inclusion of AdoHcy in saturating amounts would displace any latent AdoMet copurifying with *E. coli*-expressed VP39 (*25*) due to AdoHcy's tighter binding (*22*) and, as an MTase inhibitor, eliminate the possibility of spurious 2′-O-methylation during the experiment that might arise from contaminating AdoMet.

^{13}C2′ peaks for the four samples were assigned using 5′-rGMP (Figure 2C) as a reference. Values were scrutinized in the ^{13}C dimension initially, due to its resolution being greater than that of the ^{1}H dimension (δ_{max} for 2′-^{1}H and 1′-^{13}C being ∼0.16 and 1.6 ppm, respectively). Moreover, since 2′-proton signals lay very close to those for water, and the water content of the RNA−protein complexes was significantly higher than that of GMP, proton signals were susceptible to water suppression. C2′ δ values, plotted against pH (Figure 3A), were pH-insensitive over the range of 6.25−8.60. This result was reproducible in replicate experiments (not shown). pH insensitivity was not unexpected for the free RNA sample, insofar as the pK_a of the guanosine 2′-OH moiety within a GpA dinucleotide (identical to the ^{13}C-enriched linkage of the [^{13}C]G-RNA examined here) is 12.71 (*19*), well outside the pH range of our titration, and 2′-OH pK_a values for all RNA phosphodiester linkages lie within the range of 12.17−13.59 (ref *18* and references therein). Our incorporation of adenosine phosphorothioates in place of monophosphates was not considered to be likely to skew these values significantly. The finding of pH insensitivity for the VP39-saturated RNA samples in the pH range of 6.25−8.60 indicated an absence of VP39-induced 2′-oxyanion formation over the range of its enzymatic pH optimum. Signals for the four remaining ribose carbons (1′ and 3′−5′) also showed no pH-dependent shifts in any of the four samples (data not shown).

The coordinated pH dependence of ^{1}H and ^{13}C δ values was a hallmark of experiments with ^{13}C-enriched 5′-rGMP (Figure 2C, data not shown). To determine whether the very small variations in δ with pH observed for RNA C2′ peaks (Figure 3A) were systematic, they were examined for covariation with corresponding ^{1}H δ values (data not shown) from the same spectra. The absence of covariation (Figure 3B) indicated that the small variations were noise only, and therefore insignificant.

At the end of each HSQC experiment, RNA was recovered and its integrity confirmed (see the Supporting Information).

Effect of Ionic Strength and pH on VP39−[^{13}C]G-RNA Interaction and RNA Stability. At a concentration of ∼0.4 mM, VP39 and RNA ligand were individually soluble in NMR buffer and yielded well-resolved NMR proton spectra. However, since the protein−RNA complex required an elevated ionic strength to retain solubility at this concentration (data not shown), NMR experiments (Figure 3) contained 0.25 M $(NH_4)_2SO_4$. Since VP39 MTase activity is progressively inhibited by NaCl at concentrations greater than 50−100 mM (*22*), the effect of 0.25 M $(NH_4)_2SO_4$ upon VP39−RNA substrate interaction was investigated (and the effect of phosphorothio substitution was simultaneously investigated), by examining VP39's k_m^{RNA} under conditions prevailing in the NMR tube at the midpoint of pH titration [phosphorothio-substituted RNA in 250 mM $(NH_4)_2SO_4$ at pH 7.5], and a value of 112 μM was obtained. As confirmation that k_m^{RNA} approximates k_d for the protein−RNA interaction, isothermal titration calorimetry was also employed (data not shown), leading to k_d values in the range of 70−100 μM. At a k_d of 90 μM along with RNA and protein concentrations of 320 μM, >60% of the RNA ligand would be expected to be in the protein-bound form at equilibrium in the NMR tube. Even if k_d^{RNA} were elevated 3−10-fold at the higher pH values in the experiment [8.0 and 8.6 (*35*)], >30−40% of the ligand would nonetheless be in the protein-bound form, well above the detection limit of HSQC.

DISCUSSION

Of the >120 species of AdoMet-dependent MTase that have been assigned an EC number, approximately half methylate an oxygen (*2*). As described above (introductory section), the known 3D structure of VP39's catalytic center

with the substrate and cofactor bound affords an opportunity to examine the enzymatic mechanism of O-methylation. In the VP39 catalytic center, the target oxygen nucleophile, methyl center, and leaving group are very well aligned for an S_N2 reaction mechanism (*33*; Figure 1). Although such a mechanism has not been formally proven for VP39, the vast majority of known MTases exhibit an S_N2 mechanism as evidenced by stereochemical inversion at the methyl center (*43*). Insofar as a carbocationic methyl intermediate would be highly unstable (due to an absence of electron-donating substitutions to distribute the charge deficiency), those few MTases that appear not to undergo inversion (*43*) likely do not employ an S_N1 mechanism but instead experience a double inversion.

Although metal ions may play a role in 2′-OH deprotonation by phosphoryl transferase enzymes and ribozymes (introductory section), the roles of metals in the RNA 2′-*O*-MTase FtsJ/RrmJ are likely in substrate binding and folding as opposed to catalysis (*44*), and VP39 is entirely metal-independent. In VP39, the ϵ-amino group of the lysine 175 side chain (a critical and essential side chain for MTase catalytic activity; C. Li and P. D. Gershon, manuscript in preparation) is uniquely positioned at the MTase catalytic center to act as a general base that has been suggested to act in deprotonating the 2′-OH, providing a nucleophilic 2′-oxyanion for in-line attack on the AdoMet methyl center (*33*). The equivalent lysine in 2′-*O*-MTase FtsJ/RrmJ has also been proposed to act in 2′-OH deprotonation (*44*). Certainly, protein acid/base chemistry is adequate for abstraction of a proton from groups with pK_a values even higher than that of an aliphatic hydroxyl, with only indirect involvement of a metal ion [for example, abstraction of an α-proton from a saturated carbon center (p$K_a \sim 29$) by mandelate racemase (ref *45* and references therein)].

An enzyme-activated (deprotonated) 2′-OH would be detected in HSQC experiments as a difference between free and bound RNA in δ for the target ^{13}C2′, and a downfield shift in δ with pH over the active pH range of the enzyme due to the activation of K175 as a general base. However, despite bringing *in vitro* conditions perhaps as close as possible to a natural "poised state" at the VP39 catalytic center without effecting catalysis, we did not observe protein effects on δ (Figure 3A). An alternative mechanism might involve a less dramatic role for hydrogen bonding between K175 and the 2′-OH proton in lowering the activation energy of catalysis, via some form of partial deprotonation [bond polarization and/or stretching, perhaps via formation of a low-barrier hydrogen bond (*46*) and/or a catalytic dyad (*47*)]. While the very small downfield shift of 2′-^{13}C δ observed for all three RNA substrate-bound complexes with respect to the free substrate (Figure 3B) could be consistent with such a mechanism, this mechanism would also require K175 to be in the deprotonated form at the pH optimum of the enzyme [pH 7.5 (*22*)] and would therefore likely be pH-dependent over the pH range of 6.25−8.60 (unless K175's pK_a were depressed by ≥4 pH units from its natural value of 10.1, a degree of perturbation that is considered unlikely). The pH dependence of the small downfield shift in δ over the pH range of 6.25−8.60 was not observed (Figure 3B), arguing against the alternative mechanism.

A second alternative mechanism might involve the "capture" by VP39 of a transiently deprotonated 2′-oxyanion intermediate occurring during the naturally rapid exchange of hydroxyl protons with solvent, and a role for VP39's lysine 175 in stabilizing the captured oxyanion prior to nucleophilic attack on the AdoMet methyl. Again, HSQC experiments would be expected to reveal a downfield shift in 2′-^{13}C δ for the protein-bound RNA with respect to the coalesced signal for free RNA, only this time there would be no requirement for the downfield shift to be pH-sensitive over the pH range employed in Figure 3A insofar as the active form of lysine 175 would be the acidic one, the form naturally predominant at all pH values below the natural pK_a of 10.1. The small, pH-independent difference between free and bound observed in Figure 3B was not sufficiently great to be attributable to a fully deprotonated hydroxyl [which is apparent from the superimposed 1D spectrum of the 5′-rGMP control (Figure 3A)]. The observed data (Figure 3) are therefore inconsistent with the second alternative mechanism.

One possible drawback with each of the three mechanisms outlined above might be that they each involve, to varying degrees, electron withdrawal from the nucleophile in a direction away from the hydroxyl oxygen orbital attacking the cofactor methyl. This may be expected to decrease (or at least not to enhance) the nucleophilicity of the 2′-oxyanion toward the target methyl and therefore not to be optimal for catalysis. A third alternative mechanism is therefore proposed for enzyme-catalyzed 2′-O-methylation, one which seems to be the most consistent with the data of Figure 3A, and which stipulates no change in the protonation or polarization status of the target ribose 2′-OH prior to the commencement of nucleophilic attack. According to this mechanism, methyl group transfer is catalyzed by formation of a non-deprotonating hydrogen bond between VP39's K175 side chain and the 2′-OH proton, freezing rotation of the latter and steering an oxygen lone pair of the 2′-OH directly toward the methyl center. The 2′-OH proton would be lost at some point either at the same time as or immediately following covalent bond formation between the substrate 2′-O and the cofactor methyl. Simultaneous loss would presumably be more thermodynamically favorable to the forward methylation reaction. Even if an absence of a preparatory 2′-oxyanion formation step were less than optimal thermodynamically for MTase activity (resulting perhaps in a relatively high activation energy for the forward reaction), this would not be inconsistent with VP39's known MTase kinetics in which chemical steps appear to be slow [∼10 min per turnover under *in vitro* methylation conditions (*37*)].

Certainly, orbital steering mechanisms have been invoked in the past to account for the catalytic power of enzymes and structural incongruities in ribozyme catalytic centers (refs *48* and *49* and references therein). The orbital steering mechanism suggested herein for VP39 may be augmented by additional factors such as (a) extremely high local concentrations (and mutual proximity) of the substrate 2′-OH and methyl donor (AdoMet) at the catalytic center, (b) a destabilized ground state for the reaction due to the thermodynamic instability of AdoMet [which may be viewed as an ATP-activated form of methionine (*50*) with a charged, trivalent sulfur attached to a highly reactive donor methyl], and (c) the excellence of AdoHcy as a leaving group due to its dialkyl sulfide character. Although additional insights into VP39's mechanism could likely be gained via approaches such as the measurement of solvent deuterium kinetic isotope

effects, the precision with which VP39's kinetic rates can currently be measured has proven to be inadequate for such measurements.

An orbital steering mechanism is favored not only by its consistency with the data of Figure 3 but also by the appropriate orientation of the K175 side chain in the enzyme−substrate−cofactor complex (Figure 1). To act as an acceptor for the critical hydrogen bond from the RNA 2′-OH proton, the K175 side chain would need to be in its deprotonated state at the pH optimum of the enzyme, implying a depressed pK_a for its ϵ-amino group. Although this is perfectly feasible, the detection of K175's pK_a is beyond the scope of this study. Nonetheless, since a conserved and essential lysine corresponding to VP39's K175 seems to be a general feature of the RNA 2′-*O*-MTase catalytic center (*32*, *44*, *51*), our proposed mechanism may be applicable to the entire RNA 2′-*O*-methyltransferase family.

ACKNOWLEDGMENT

We thank Dr. Z. Peng for preliminary studies, Dr. J. Chattopadhyaya for discussion of ^{13}C electron shielding effects and the anomeric effect, and Dr. Alec E. Hodel (deceased) for providing VP39 expression plasmid ΔCHis. This work is dedicated to the memory of Dr. Alec E. Hodel.

SUPPORTING INFORMATION AVAILABLE

Additional experimental details, generation of [^{13}C]G-RNA (Figure 1), and RNA integrity at the conclusion of each 48 h HSQC experiment (Figure 2). This material is available free of charge via the Internet at http://pubs.acs.org.

REFERENCES

1. Cheng, X., and Blumenthal, R. M. (1999) *S-Adenosylmethionine-dependent methyltransferases: Structures and Functions*, World Scientific, Singapore.
2. Fauman, E. B., Blumenthal, R. M., and Cheng, X. (1999) in *Structure and function of AdoMet-dependent methyltransferases* (Cheng, X., and Blumenthal, R. M., Eds.) pp 1−38, World Scientific Publishing Co./Imperial College Press, Singapore.
3. Bachellerie, J.-P., and Cavaillé, J. (1997) Guiding ribose methylation of rRNA, *Trends Biochem. Sci. 22*, 257−261.
4. Bachellerie, J. P., and Cavaillé, J. (1998) in *Modifying and editing of RNA* (Grosjean, H., and Benne, R., Eds.) pp 255−272, American Society for Microbiology, Washington, DC.
5. Tycowski, K. T., You, Z.-H., Graham, P. J., and Steitz, J. A. (1998) Modification of U6 spliceosomal RNA Is guided by other small RNAs, *Mol. Cell 2*, 629−638.
6. Kiss-Laszlo, Z., Henry, Y., Bachellerie, J.-P., Caizergues-Ferrer, M., and Kiss, T. (1996) Site-specific ribose methylation of preribosomal RNA: a new function for small nucleolar RNAs, *Cell 85*, 1077−1088.
7. Usher, D. A., Richardson, D. I. J., and Oakenfull, D. G. (1970) Models of ribonuclease action. II. Specific acid, specific base, and neutral pathways for hydrolysis of a nucleaotide diester analog, *J. Am. Chem. Soc. 92*, 4699−4712.
8. Pelletier, H., Sawaya, M. R., Kumar, A., Wilson, S. H., and Kraut, J. (1994) Structures of ternary complexes of rat polymerase β, a DNA template-primer, and ddCTP, *Science 264*, 1891−1903.
9. Steitz, T. A. (1999) DNA polymerases: Structural diversity and common mechanisms, *J. Biol. Chem. 274*, 17395−17398.
10. Lott, W. B., Pontius, B. W., and von Hippel, P. H. (1998) A two-metal ion mechanism operates in the hammerhead ribozyme-mediated cleavage of an RNA substrate, *Proc. Natl. Acad. Sci. U.S.A. 95*, 542−547.
11. Steitz, T. A., and Steitz, J. A. (1993) A general two-metal-ion mechanism for catalytic RNA, *Proc. Natl. Acad. Sci. U.S.A. 90*, 6498−6502.
12. Narlikar, G. J., and Herschlag, D. (1997) Mechanistic aspects of enzymatic catalysis: Lessons from comparison of RNA and protein enzymes, *Annu. Rev. Biochem. 66*, 19−59.
13. Kim, E. E., and Wyckoff, H. W. (1991) Reaction mechanism of alkaline phosphatase based on crystal structures. Two-metal ion catalysis, *J. Mol. Biol. 218*, 449−464.
14. Hegazi, M. F., Borchard, R. T., and Schowen, R. L. (1976) SN2-like transition state for methyl transfer catalyzed by catechol-O-methyl-transferase, *J. Am. Chem. Soc. 98*, 3048−3049.
15. Vidgren, J., Svensson, L. A., and Liljas, A. (1994) Crystal structure of catechol *O*-methyltransferase, *Nature 368*, 354−358.
16. Vidgren, J., Ovaska, M., Tenhunen, J., Tilgmann, C., Lotta, T., and Mannisto, P. T. (1999) in *Structure and function of AdoMet-dependent methyltransferases* (Cheng, X., and Blumenthal, R. M., Eds.) pp 55−91, World Scientific Publishing Co./Imperial College Press, Singapore.
17. Dawson, R. C., Elliott, D. C., Elliott, W. H., and Jones, K. M. (1994) *Data for Biochemical Research*, 3rd ed., Clarendon Press, Oxford, U.K.
18. Velikyan, I., Acharya, S., Trifonova, A., Foldesi, A., and Chattopadhyaya, J. (2001) The pK_a's of 2′-hydroxyl group in nucleosides and nucleotides, *J. Am. Chem. Soc. 123*, 2893−2894.
19. Acharya, S., Foldesi, A., and Chattopadhyaya, J. (2003) The pK_a of the internucleotidic 2′-hydroxyl group in diribonucleoside (3′→5′) monophosphates, *J. Org. Chem. 68*, 1906−1910.
20. Knipe, J. O., and Coward, J. K. (1979) Role of buffers in a methylase model reaction. General base catalysis by oxyanions vs. nucleophilic dealkylation by amines, *J. Am. Chem. Soc. 101*, 4339−4348.
21. Knipe, J. O., Vasquez, P. J., and Coward, J. K. (1982) Methylase models: Studies on general-base vs. nucleophilic catalysis in the intramolecular alkylation of phenols, *J. Am. Chem. Soc. 104*, 3202−3209.
22. Barbosa, E., and Moss, B. (1978) mRNA(nucleoside-2′-)-methyltransferase from vaccinia virus: Characteristics and substrate specificity, *J. Biol. Chem. 253*, 7698−7702.
23. Barbosa, E., and Moss, B. (1978) mRNA(nucleoside-2′-)-methyltransferase from vaccinia virus: Purification and properties, *J. Biol. Chem. 253*, 7692−7697.
24. Schnierle, B. S., Gershon, P. D., and Moss, B. (1992) Cap-specific mRNA (nucleoside-$O^{2'}$-)-methyltransferase and poly(A) polymerase stimulatory activities of vaccinia virus are mediated by a single protein, *Proc. Natl. Acad. Sci. U.S.A. 89*, 2897−2901.
25. Hodel, A. E., Gershon, P. D., Shi, X., and Quiocho, F. A. (1996) The 1.85 Å structure of vaccinia protein VP39: A bifunctional enzyme that participates in the modification of both mRNA ends, *Cell 85*, 247−256.
26. Hodel, A. E., Gershon, P. D., Shi, X., Wang, S.-M., and Quiocho, F. A. (1997) Specific protein recognition of an mRNA cap through its alkylated base, *Nat. Struct. Biol. 4*, 350−354.
27. Michel, G., Sauvé, V., Larocque, R., Li, Y., Matte, A., and Cygler, M. (2002) The Structure of the RlmB 23S rRNA Methyltransferase Reveals a New Methyltransferase Fold with a Unique Knot, *Structure 10*, 1303−1315.
28. Reinisch, K. M., Nibert, M., and Harrison, S. C. (2000) Structure of the reovirus core at 3.6 Å resolution, *Nature 404*, 960−967.
29. Tao, Y., Farsetta, D. L., Nibert, M., and Harrison, S. C. (2002) RNA Synthesis in a Cage: Structural Studies of Reovirus Polymerase λ3, *Cell 111*, 733−745.
30. Egloff, M.-P., Benarroch, D., Selisko, B., Romette, J.-L., and Canard, B. (2002) An RNA cap (nucleoside-2′-O-)-methyltransferase in the flavivirus RNA polymerase NS5: crystal structure and functional characterization, *EMBO J. 21*, 2757−2768.
31. Bugl, H., Fauman, E. B., Staker, B. L., Zheng, F., Kushner, S. R., Saper, M. A., Bardwell, J. C., and Jakob, U. (2000) RNA methylation under heat shock control, *Mol. Cell 6*, 349−360.
32. Ferron, F., Longhi, S., Henrissat, B., and Canard, B. (2002) Viral RNA-polymerases: a predicted 2′-O-ribose methyltransferase domain shared by all Mononegavirales, *Trends Biochem. Sci. 27*, 222−224.
33. Hodel, A. E., Gershon, P. D., and Quiocho, F. A. (1998) Structural basis for sequence non-specific recognition of 5′-capped mRNA by a cap modifying enzyme, *Mol. Cell 1*, 443−447.
34. Peng, Z.-H., Sharma, V., Singleton, S., and Gershon, P. D. (2002) Synthesis and application of a chain-terminating dinucleotide mRNA cap analog, *Org. Lett. 4*, 161−164.
35. Lockless, S. W., Cheng, H.-T., Hodel, A. E., Quiocho, F. A., and Gershon, P. D. (1998) Recognition of capped RNA substrates by

VP39, the vaccinia virus-encoded mRNA cap-specific 2′-O-methyltransferase, *Biochemistry 37*, 8564−8574.
36. Schnierle, B. S., Gershon, P. D., and Moss, B. (1994) Mutational analysis of a multifunctional protein, with mRNA 5′ cap-specific (nucleoside-2′-O-)-methyltransferase and 3′-adenylyltransferase stimulatory activities, encoded by vaccinia virus, *J. Biol. Chem. 269*, 20700−20706.
37. Hu, G., Oguro, A., Li, C., Gershon, P. D., and Quiocho, F. A. (2002) The "cap-binding slot" of an mRNA cap-binding protein: Quantitative effects of aromatic side chain choice in the double-stacking sandwich with cap, *Biochemistry 41*, 7677−7687.
38. Horsley, W. J., and Sternlicht, H. (1968) Carbon-13 magnetic resonance studies of amino acides and peptides, *J. Am. Chem. Soc. 90*, 3738−3748.
39. Quirt, A. R., Lyerla, J. R. J., Peat, I. R., Cohen, J. S., Reynolds, W. F., and Freedman, M. H. (1974) Carbon-13 nuclear magnetic resonance titration shifts in amino acids, *J. Am. Chem. Soc. 96*, 570−574.
40. Saenger, W. (1984) *Principles of Nucleic Acid Structure*, Springer-Verlag, New York.
41. Luptak, A., Ferre-D'Amare, A. R., Zhou, K., Zilm, K. W., and Doudna, J. A. (2001) Direct pK_a measurement of the active-site cytosine in a genomic hepatitis delta virus ribozyme, *J. Am. Chem. Soc. 123*, 8447−8452.
42. Gao, X., and Jeffs, P. W. (1994) NMR studies of a hybrid DNA-RNA dodeca-duplex. 3D NOESY-NOESY spectral analysis and sequence dependent conformational heterogeneity, *J. Biomol. NMR 4*, 367−384.
43. Floss, H. G., and Tsai, M.-D. (1979) Chiral methyl groups, *Adv. Enzymol. 50*, 243−302.
44. Hager, J., Staker, B. L., Bugl, H., and Jakob, U. (2002) Active site in RrmJ, a heat shock-induced methyltransferase, *J. Biol. Chem. 277*, 41978−41986.
45. Kenyon, G. L., Gerlt, J. A., Petsko, G. A., and Kozarich, J. W. (1995) Mandelate Racemase: Structure−function studies of a pseudosymmetric enzyme, *Acc. Chem. Res. 28*, 178−186.
46. Ha, N.-C., Kim, M.-S., Lee, W., Choi, K. Y., and Oh, B.-H. (2000) Detection of large pK_a perturbations of an inhibitor and a basis for catalytic power of many enzymes, *J. Biol. Chem. 275*, 41100−41106.
47. Paetzel, M., and Dalbey, R. E. (1997) Catalytic hydroxyl/amine dyads within serine proteases, *Trends Biochem. Sci. 22*, 28−31.
48. Mesecar, A. D., Stoddard, B. L., and Koshland, D. E. J. (1997) Orbital steering in the catalytic power of enzymes: small structural changes with large catalytic consequences, *Science 277*, 202−206.
49. Scott, W. G. (2001) Ribozyme catalysis via orbital steering, *J. Mol. Biol. 311*, 989−999.
50. Cantoni, G. L. (1952) The nature of the active methyl donor formed enzymatically from L-methionine and adenosine triphosphate, *J. Am. Chem. Soc. 74*, 2942−2943.
51. Bujnicki, J. M., and Rychlewski, L. (2002) In silico identification, structure prediction and phylogenetic analysis of the 2′-O-ribose (cap 1) methyltransferase domain in the large structural protein of ssRNA negative-strand viruses, *Protein Eng. 15*, 101−108.
52. Luyten, I., Thibaudeau, C., and Chattopadhyaya, J. (1997) The Strength of the Anomeric Effect in Adenosine, Guanosine, and in Their 2′-Deoxy Counterparts is Medium-Dependent, *J. Org. Chem. 62*, 8800−8808.

BI0359980